PROCEEDINGS, 47th Workshop on Geothermal Reservoir Engineering
Stanford University, Stanford, California, February 7-9, 2022
SGP-TR-223

Managing Injection Parameters to Control Hydraulic Fracture Patterns

Wenfeng Li, Luke P. Frash, J. William Carey, Meng Meng, Nathan J Welch

Los Alamos National Laboratory, TA03-40-S5, MS D462, Los Alamos, NM 87545

wenfeng@lanl.gov

Keywords: EGS, Hydraulic Fracture Branching, Optimization, Injection Design

ABSTRACT

Hydraulic fracturing is a key technology that can increase the permeability of a hot dry rock reservoir to an economically viable level for effective heat extraction. It is crucial to create fracture networks in the subsurface for sustained heat production. Previous studies have shown that hydraulic fractures can grow in planar structures or branch into multiple strands. However, it is unclear what conditions and injection design can lead to complex fracture patterns. To address this, we conducted laboratory hydraulic fracturing experiments using analog-rock samples that were constructed with controlled heterogeneity for repeatable experiments. We employed different combinations of injection rates and fracturing fluid viscosities to fracture the heterogeneous samples. The results indicate that: a) Slow injection of low-viscosity fluids results in diffusion-dominated fluid flow; 2) Injection of medium-viscosity fluids at moderate rate leads to complex fracture networks via crack branching; 3) Fast injection of high-viscosity fluid causes planar hydraulic fracture pattern. Those experimental results are repeatable, which suggests that manipulating injection rates and fluid viscosities allows us to control hydraulic fracture patterns in rock formations with pre-existing and permeable weak layers. For application in the field, our results can help to optimize injection fluid properties to create complex hydraulic fracture networks for sustained heat production from geothermal reservoirs.

1. INTRODUCTION

Since early 1970s, significant amount of efforts has been made to develop Enhanced Geothermal System (EGS) for effective heat extraction in deep non-volcanic regions (Breede et al., 2013). The EGS concept typically requires drilling of multiple wells into the hot crystalline basement and circulating fluid through injection and production wells for heat extraction. The natural hot crystalline basement is often not permeable enough for efficient heat extraction, therefore, hydraulic stimulation is necessary to significantly improve reservoir permeability for economic viability (Frash et al., 2014). Hydrofracturing and hydroshearing are two effective engineering measures for enhancement of reservoir permeability, the former refers to the creation of new fractures or reopen natural ones while the latter aims to slide pre-existing fractures with shear dilation for permeability improvement. Hydroshearing favors permeable, weakly cohesive, and properly-oriented natural fractures, as demonstrated by laboratory and field studies (Guglielmi et al., 2015; Meng et al., 2022). In many cases, hydrofracturing can occur simultaneously as hydroshearing because of the excess injection pressure (McClure and Horne, 2014; Rinaldi and Rutqvist, 2019; Frash, 2022). It is, therefore, important to understand hydraulic fracture initiation and propagation for effective development of EGS reservoirs.

Complex fracture patterns in an EGS reservoir are desired because they can significantly increase the fluid-rock contact areas for heat exchange. Although hydroshearing cannot be excluded, hydrofracturing has been reported to successfully create complex fracture patterns in deep subsurface, e.g. at the hydraulic fracturing testing site (Gale et al., 2018). This motivates the research interest that whether we can promote complex hydraulic fractures under the subsurface conditions by managing controllable engineering parameters, such as the injection design, which forms the focus of the present study.

Pioneer study has been done by Renshaw and Pollard (1995) for investigation of hydraulic fracture propagation in heterogeneous rocks (Fig. 1). They proposed the well-known crossing/arresting criterion of a hydraulic fracture when approaching a pre-existing weak layer and validated their theory based on a series of excellent experiments. Many subsequently studies were conducted by other researchers for more complete investigations of crossing/arresting of hydraulic fractures, including the effect of approaching angle of the hydraulic cracks (Weng et al., 2011) and the degrees of weak layer cementation (Fu et al., 2018). However, Renshaw and Pollard, as well as the subsequent studies, did not account for fluid flow and pressure on the opening of pre-existing weak layers, which is the main reason that their theory is not applicable to explain hydraulic fracture branching that depicts simultaneous propagation of hydraulic fractures in multiple directions (Fig. 1). Stress states of rock matrix near the hydraulic fractures can change via poroelastic and effective stress responses during transient fluid flow and pressure diffusion at hydraulic fracture walls.

Hydraulic fracture branching is a complex result of reservoir conditions and the injection parameters. In-situ stress condition is probably the most important factor because strong anisotropic in-situ stresses favor near-planar hydraulic cracks whereas weak stress anisotropy can promote crack branching. Hydromechanical properties of pre-existing weak layers also determine the likelihood of occurrence of opening of pre-existing weak layers. In addition, fracturing fluid viscosity and injection rate can also influence hydraulic crack patterns, as demonstrated in laboratory experiments (Ishida et al., 2004; Tan et al., 2017). While studies have revealed those influencing factors on the resultant hydraulic crack patterns, it is poorly understood what combination of engineering/controllable parameters will lead to distinct hydraulic crack patterns in the subsurface.

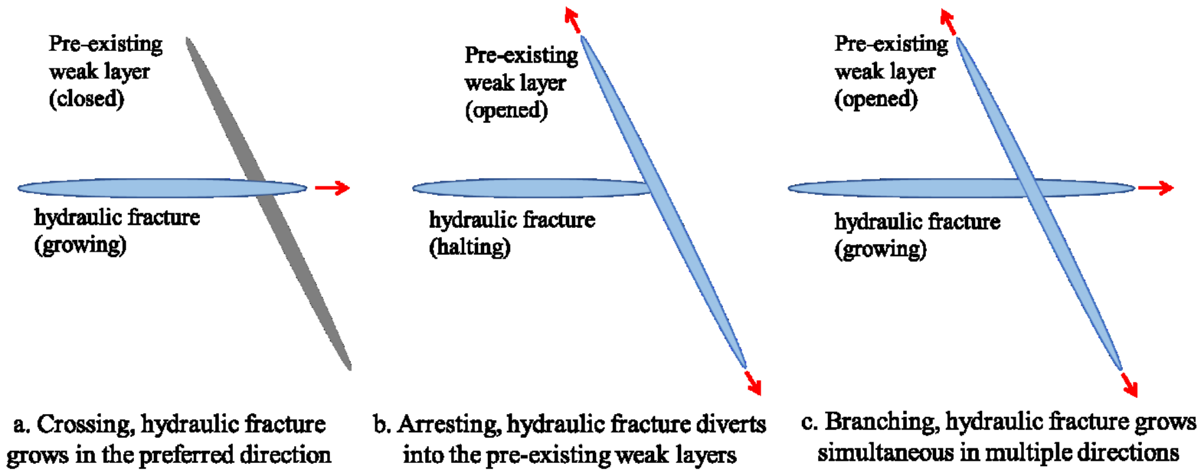

Figure 1: Hydraulic fracture interaction with pre-existing weak layers. The theory proposed by Renshaw and Pollard (1995) focuses crossing (a) and arresting (b) of hydraulic cracks, but is not applicable to explain hydraulic fracture branching (c) that results from transient fluid flow and pressure diffusion at hydraulic crack walls.

In this study, we investigate the effect of controllable injection parameters, e.g., injection rate and fracturing fluid viscosity, on hydraulic fracture patterns using analog-rock samples. The analog-rock samples include controllable and repeatable heterogeneous structures to represent rock mass with pre-existing weak layers in the subsurface. We analyze the interplay among the injection design, sample stress states, and the hydromechanical properties of the rock matrix and the pre-existing weak layers, aiming to identify the critical injection designs that result in distinct resultant crack patterns. Our study can shed light on the optimization of injection design to promote complex hydraulic fracture networks in the subsurface.

2. EXPERIMENTAL DESIGN AND HYDROMECHANICAL CHARACTERIZATION OF SAMPLES

We use plaster of Paris to cast the analog-rock samples of controlled heterogeneity (Fig. 2). In order to mimic naturally fractured rock mass, we cast the weak layers using plaster-water ratio of 100:100. We then fill the grids using plaster:water ratio of 180:100, which represents the rock matrix. The whole sample is cast inside a steel ring with a wall thickness of 9.5 mm and a diameter of 304.8 mm. We then installed four biaxial strain gauges at the outside wall of the steel ring for tangential strain measurements. The sample has an average thickness of 27.94 mm. Note that we used plaster samples, instead of natural rocks, in the experiments because we wanted to well control the heterogeneous structures and the hydromechanical properties of the samples, which enables systematic and repeatable investigation of the influence of injection parameters on the hydraulic crack patterns.

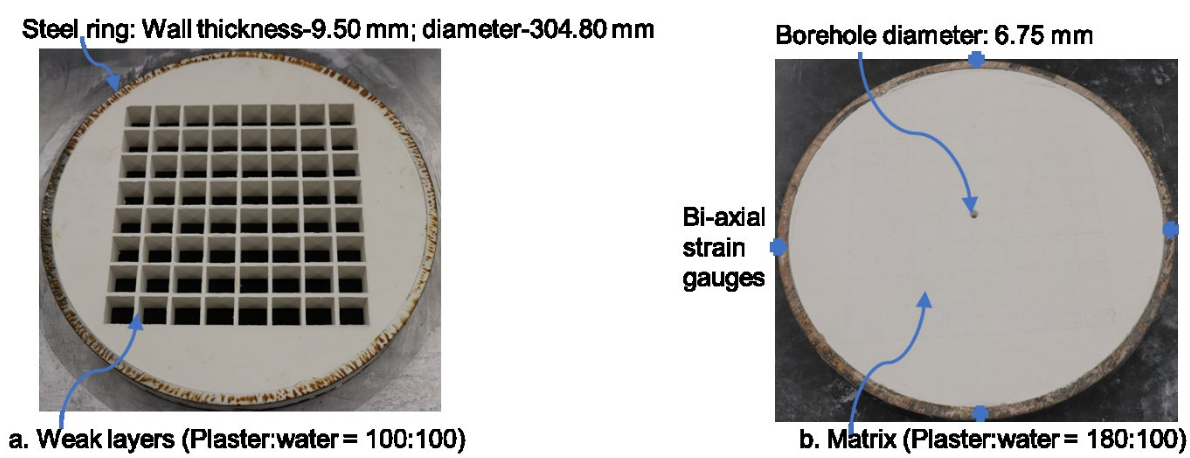

Figure 2: Analog-rock samples of controlled heterogeneity for repeatable hydraulic fracturing experiments. We first cast the weak layers using plaster-water ratio of 100:100 (left), after which plaster-water ratio of 180:100 was used to fill the grids that represent the rock matrix.

In order to facilitate theoretical development and numerical modeling, we also measured the hydromechanical properties of the plaster-water mixtures using relevant batch tests. The measured properties are summarized in Table 1. For the fracture energy measurements, we prepared beam samples of three different sizes to account for the size effect (Bažant and Planas, 2019). We also measured the Biot effective stress coefficient for each plaster-water mixture using the constant volumetric method in a triaxial system, detailed test procedures can be found in Meng et al. (2020).

Table 1: Physical and hydromechanical properties of the analog-rock samples.

Plaster/water ratio (wt%)	180:100	100:100	Note
Dry density (g/cm^3)	1.21	0.85	-
Porosity (%)	38.9	55.5	Saturation-drying test
Young's modulus (GPa)	7.72	1.37	Uniaxial compression test
Poisson's ratio	0.044	0.088	
Uniaxial compressive strength (MPa)	10.65	3.79	
Tensile strength (MPa)	2.04	1.18	Brazilian test
Permeability (md)	27.08	87.83	Core-flooding test
Specific fracture energy (N/m)	4.27	2.49	Three-point bending
Biot effective stress coefficient	0.82	0.94	Constant deformation method

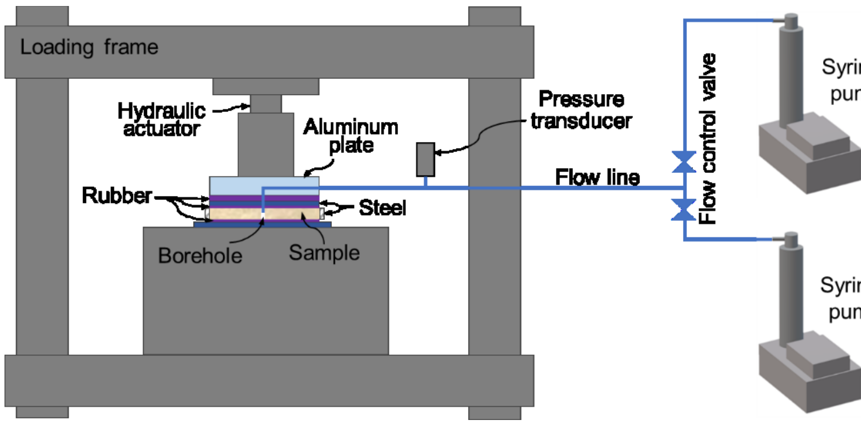

Figure 3: Setup of the hydraulic fracturing experiments. Axial stress is applied through hydraulic actuator in the vertical direction before fluid injection. The sample was sandwiched by rubber layers on the top and bottom for fluid seal. Syringe pumps are used to inject oils of different viscosities at various volumetric rates to hydraulically fracture the sample.

Fig. 3 shows the experimental setup for the hydraulic fracturing tests. Samples were first polished to ensure parallel surfaces. Injection borehole was drilled at the sample center, as shown in Fig. 2b. We then placed rubber sheets on the top and bottom of samples to ensure uniform vertical stress upon loading. The rubber sheets also helped to seal the injection fluid to avoid leakage at sample surfaces for greater vertical stress than the breakdown pressure of the sample. During the test, we first exerted vertical stress across the sample top, the resulting lateral deformation of the sample is restricted by the steel ring. In other words, the horizontal stress is passively generated by the Poisson's effect of the sample. Once the target vertical stress was reached, we started fluid injection by using the syringe pumps, based on which we recorded the injection rate. Although the syringe pumps also recorded the fluid pressure, we installed a pressure transducer close to the aluminum plate (Fig. 3) for hydraulic pressure recording to eliminate most of the friction loss in the flow line.

3. EXPERIMENTAL RESULTS

3.1 Heterogeneous Samples

We first injected oils of different viscosities at different volumetric rates into heterogeneous samples. All the samples have weak layers that were cast using plaster-water ratio of 100:100 and matrix of plaster-water ratio of 180:100. In other words, all the heterogeneous samples have the same heterogeneous structures and hydromechanical properties as listed in Table 1. In addition, we exerted similar axial stresses at the sample top, but used distinct injection parameters among those tests. Below we discuss three representative experiments in detail.

We observed diffusion-dominated injection when low-viscosity oil was injected at a slow volumetric rate. Fig. 4 shows one particular example for the test B04-01. We applied 3.9 MPa vertical stress on the sample top, which passively induced the lateral stress of 0.5 MPa by the steel ring. Once the vertical stress stabilized, we injected spindle oil of 8.81 cp viscosity at a constant rate of 8.4 ml/min for 21.4 mins. The injection fluid pressure maxed at 0.54 MPa, which is below the tensile strength of weak layers. The injection pressure response indicates no hydraulic fracturing, consistent with the post-experiment observation shown in Fig. 4. Therefore, this injection rate and fluid viscosity only result in radial diffusion around the injection borehole.

Using intermediate injection rate and fluid viscosity, we achieved complex hydraulic fracture pattern via crack branching in the heterogeneous samples. Fig. 5 shows one typical example (Test B05-01). Here, we applied 2.8 MPa vertical stress on the sample top and strain gauge response indicated an average lateral stress of 0.85 MPa before injection (the bottom panel in Fig. 5). Note that we calculated lateral stress using the strain gauge reading in tangential direction, based on the thick wall theory. Starting at about 500 seconds, we started the fluid leak-off test by employing a slow injection rate at 1.0 ml/min. The injected oil has a viscosity of 403.9 cp. Leak-off test indicated an injectivity index of 2.28 ml/(min·MPa), defined as the ratio between injection rate and fluid pressure difference. At ~1700 seconds, we increased the injection rate to 20.0 ml/min to hydraulically fracture the sample. The breakdown pressure occurred at 2.71 MPa, followed by some minor pressure peaks at later times that possibly indicated crack branching. Strain gauges responded consistently with breakdown pressure and the subsequent crack propagation. Post experimental observation demonstrates that complex hydraulic fracture patterns occurred, as photographed and sketched in Fig. 5.

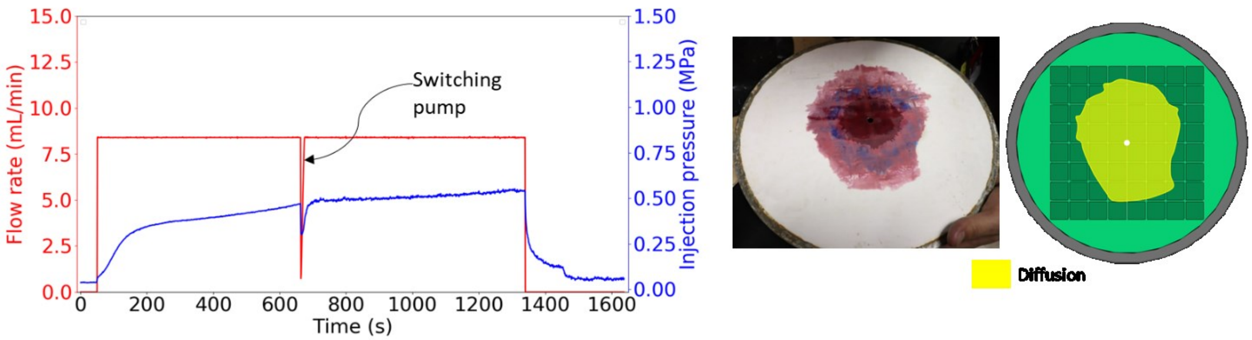

Figure 4: Experimental results of the heterogeneous sample B04-01. We injected low-viscosity oil (8.81 cp) at a volumetric rate of 8.4 ml/min, resulting in diffusion-dominated flow.

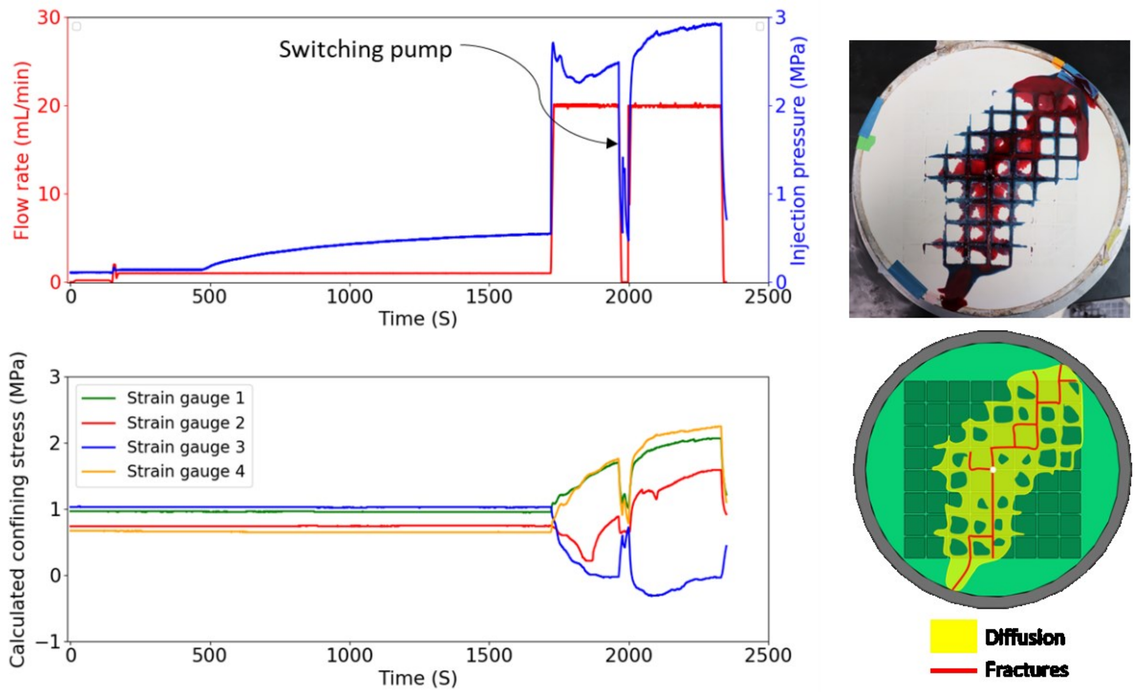

Figure 5: Experimental results of the heterogeneous sample B05-01. We injected intermediate-viscosity oil (403.9 cp) at a volumetric rate of 20.0 ml/min, resulting in complex crack network via fracture branching.

When we further increased the injection rate and fluid viscosity, we only observed planar or near-planar hydraulic fractures without crack branching in the same heterogeneous samples. Fig. 6 shows the results of such a test B05-03. Again, uniform vertical stress of 3.25 MPa was applied to the sample top, which induced passive confinement of 0.85 on average according to the strain gauge readings (bottom plot in Fig. 6). Oil of 403.9 cp viscosity was injected at 60.0 ml/min to induce hydraulic fractures. The injection pressure quickly peaked at 5.23 MPa. After sample breakdown, fluid pressure was maintained close to 4 MPa. High fluid pressure in the hydraulic cracks could have promoted hydraulic crack branching at the weak layers, but due to the short injection duration, transient pressure diffusion did not accumulate enough to open the weak layers.

We have repeated the experimental results in Figs 4 – 6 using the controllable heterogeneous samples. Fast injection of high-viscosity fluid induces planar or near-planar hydraulic fractures. Intermediate injection rate and fluid viscosity cause hydraulic fracture branching, whereas slow injection of low-viscosity fluid results in diffusion-dominated flow. Those results suggest that for heterogeneous rocks in the subsurface, we can potentially manage the injection design to control the induced hydraulic fracture patterns. For completeness, we further investigate how the sample heterogeneity affects the critical injection parameters that separate the three regimes.

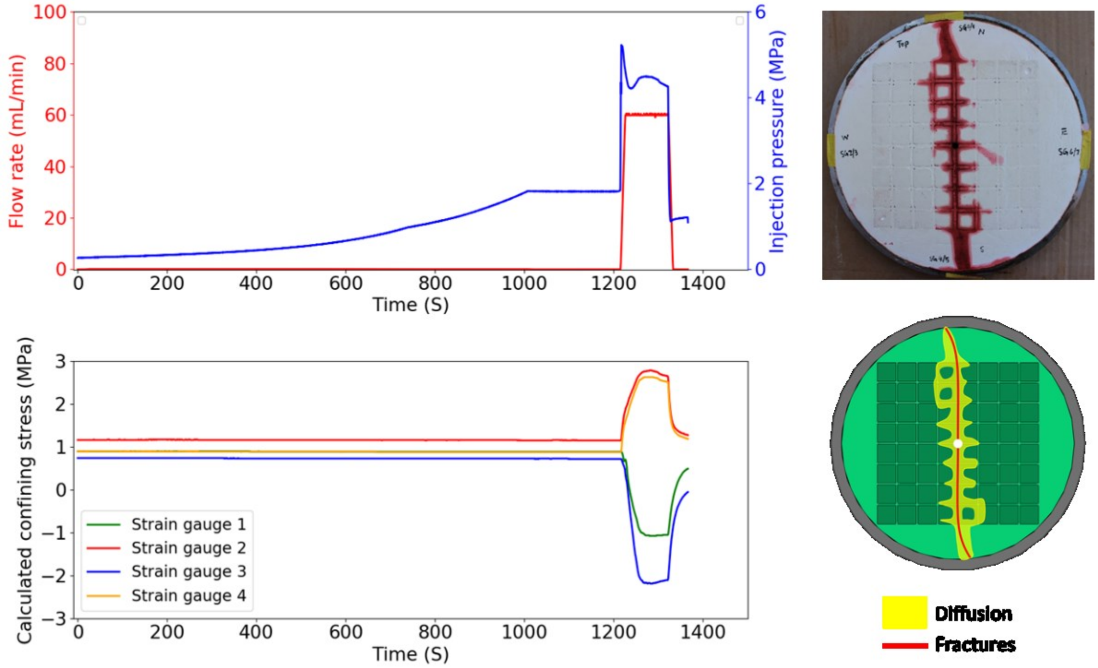

Figure 6: Experimental results of the heterogeneous sample B05-02. We injected intermediate-viscosity oil (403.9 cp) at a volumetric rate of 60.0 ml/min, resulting in simple planar hydraulic fractures.

3.2 Homogeneous Samples

We prepared some homogeneous samples that did not contain the pre-existing weak layers for further experimental investigation. The samples were cast using plaster-water ratio of 100:100 in a single cast step. Again, hydromechanical properties of the sample are summarized in Table 1. We conducted the experiments on homogeneous samples in order to investigate how the injection parameters could affect the hydraulic fracture patterns without the influence of the pre-existing weak layers. Our previous computer modeling indicated that crack branching would not occur in homogeneous samples without weak layers (Rahimi-Aghdam et al., 2019). We aimed to explore the validity of modeling results based on experiments.

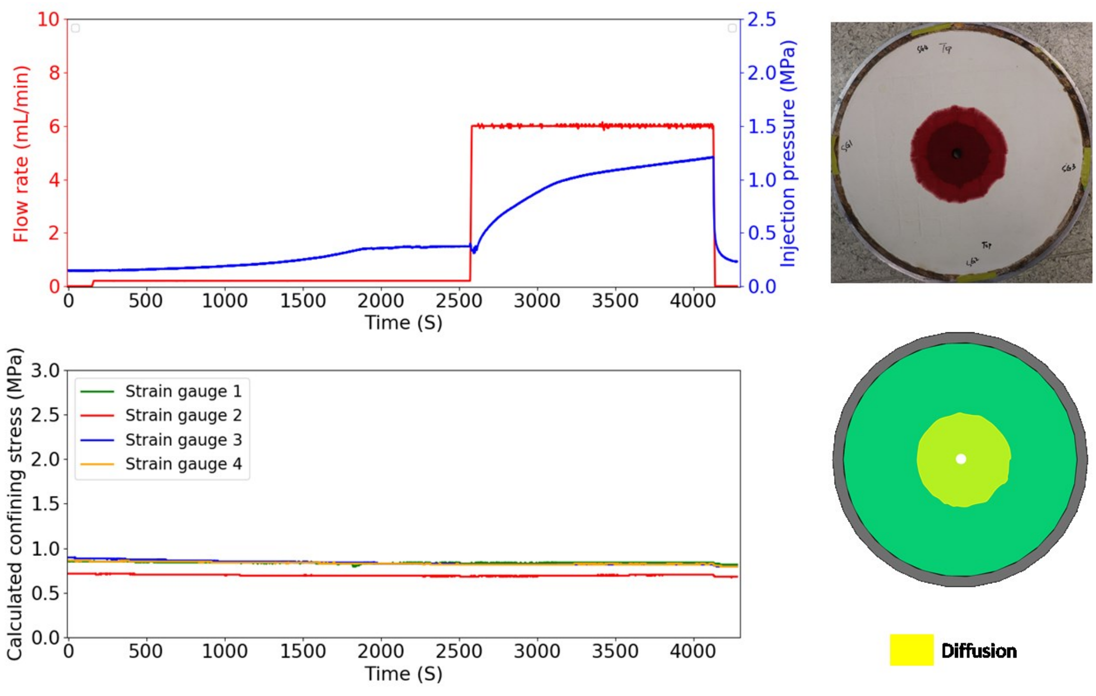

Figure 7: Experimental results of the homogeneous sample B05-03. We injected low-viscosity oil (57.8 cp) at a volumetric rate of 6.0 ml/min, resulting in diffusion dominated fluid flow.

We observed diffusion-dominated injection in homogeneous samples for slow injection of low-viscosity fluid. As shown in Fig. 7, the test B05-03 is dominated by radial diffusion. The vertical stress was exerted on sample top at 3.1 MPa, which induced an average lateral stress (or confinement) at 0.8 MPa. Following the leak-off test, we started injection of the oil, with 57.8 cp viscosity, at an injection rate of 6.0 ml/min. The injection pressure maxed at about 1.2 MPa at the end of injection, which did not hydraulically crack the sample. Therefore, slow injection of low viscosity fluid only caused diffusion-dominated results in the porous and permeable samples.

As a comparison, we conducted fluid injection into homogeneous samples at greater injection rates and fluid viscosities. Shown in Fig. 8, we observed bi-wing or near-planar hydraulic fractures for intermediate viscosity and injection rate. In this test, we exerted vertical stress at ~3.2 MPa and lateral stress of 1.1 MPa. Injection of intermediate viscosity oil (403.9 cp) was maintained at a constant rate of 20.0 ml/min. The pressure response indicated hydraulic fracturing with the breakdown pressure at ~5.4 MPa. Strain gauges also demonstrated stress changes during hydraulic fracture initiation and propagation. Shown on the right in Fig. 8, we observed multi-stranded hydraulic fractures in near-planar pattern. This injection rate and fluid viscosity could have resulted in crack branching if pre-existing weak layers were present in the sample (see Fig. 5). However, without the pre-existing weak layers, crack branching was not observed in homogeneous samples with the same injection design. This provides direct experimental evidence to our previous computer simulations that concluded pre-existing weak layers are necessary in order to encourage hydraulic fracture branching in the subsurface (Rahimi-Aghdam et al., 2019).

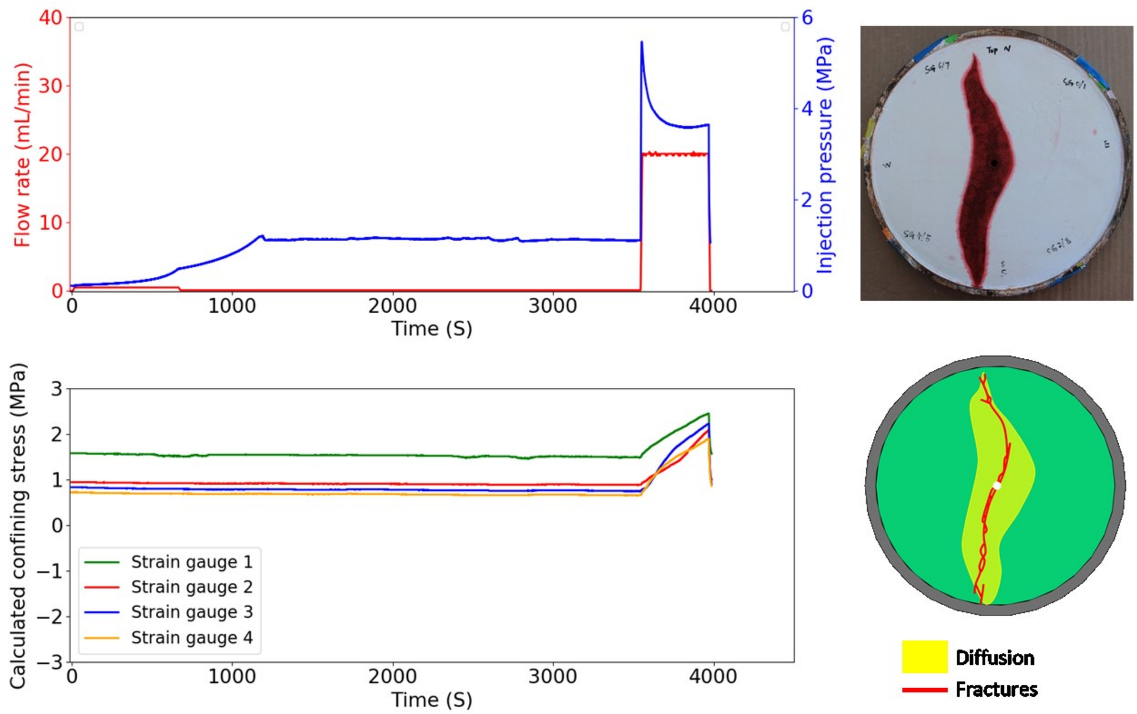

Figure 8: Experimental results of the homogeneous sample B05-03. We injected intermediate-viscosity oil (403.9 cp) at a volumetric rate of 20.0 ml/min, resulting in simple near-planar hydraulic fractures.

4. DISCUSSION

We combine all the experimental results, as shown in Fig .9, to quantify the injection parameters that separate the three regimes of fracture patterns. For each experiment, we divide the injection rate by the sample thickness to obtain the normalized injection rate in the dimension of m^2/s. As shown in Fig. 9, we combine the normalized injection rate and fluid viscosity in the vertical axis, because both terms are related to the rate of energy input into the sample. In the horizontal axis, we define the sample heterogeneity by using the permeability ratio between the weak layer and the rock matrix. We can summarize from Fig. 9 that for heterogeneous samples that contain pre-existing weak layers, small rate and fluid viscosity cause diffusion-dominated injection; intermediate rate and fluid viscosity result in fracture branching. Increasing both parameters create near-planar hydraulic fractures. The regime of hydraulic fracture branching is absent for the homogeneous samples, regardless of injection rate and fluid viscosity. The critical injection parameters are a function of the sample heterogeneity and can be computed based on the theory we proposed previously (Li et al., 2021a).

There are some simplifications in our study that need further discussion. First, we did not consider other mechanisms, such as hydroshearing of pre-existing weak layers, that can potentially affect hydraulic fracture propagation in the subsurface. Although hydroshearing cannot be excluded for hydraulic fracturing treatment, our study demonstrates that tensile opening of pre-existing weak layers can occur in the lateral direction of a hydraulic crack under three principal stresses. Second, our experiments are all under room temperature conditions. However, the experimental findings may be applicable for hydraulic fracturing treatment of elevated temperatures when thermoelastic effect is simplified as isotropic, according to the superposition principle. For rocks and weak layers of anisotropic thermoelastic behavior, further investigations are indeed necessary. Third, our experiments are conducted under isotropic horizontal stress conditions. Although this is barely relevant to the real subsurface stress condition, our theory indicates that hydraulic fracture branching can occur under certain anisotropic horizontal stress conditions, as elaborated in Li et al. (2021a). Addition work is ongoing to investigate the critical anisotropic stress states that can inhibit hydraulic fracture branching.

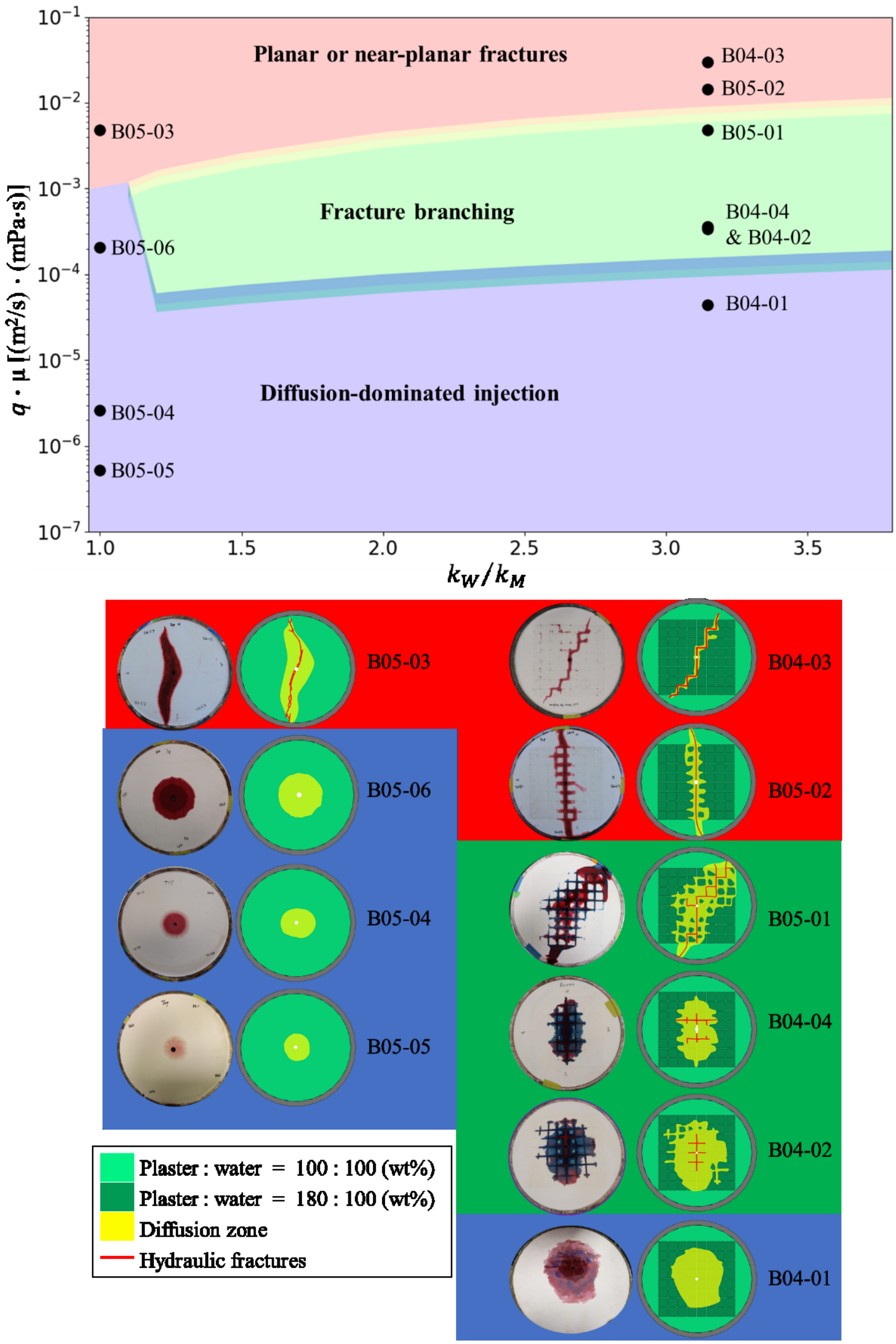

Figure 9: Effect of injection rate and fluid viscosity on hydraulic fracture patterns. For homogeneous samples (left), there are critical injection parameters that define diffusion-dominated injection versus planar-hydraulic fracturing. For heterogeneous samples (right), intermediate injection rate and fluid viscosity can promote hydraulic fracture branching, besides the diffusion-dominated case and near-planar hydraulic crack pattern.

5. CONCLUSIONS

In this study, we conducted a series of repeatable hydraulic fracturing experiments to investigate effect of injection design on the resultant hydraulic crack patterns for potential application in Enhanced Geothermal Reservoir (EGS) development. Analog-rock samples were cast to enable repeatable preparation of samples of controlled heterogeneity. We maintained similar stress conditions but purposely varied the injection rate and fracturing fluid viscosity among the experiments. When samples contain permeable, pre-existing weak layers, we demonstrated that injection is diffusion-dominated for small injection rate and fluid viscosity. Intermediate injection parameters cause hydraulic fracture branching that eventually leads to complex fracture network. Large injection parameters only result in planar or near-planar hydraulic fractures. For homogeneous samples without pre-existing weak layers, we observed diffusion-dominated injection and planar hydraulic fractures with the absence of crack branching regime. Our finding suggests that we can potentially manage the injection parameters to promote more complex fracture network in an EGS reservoir for sustained heat production.

ACKNOWLEDGMENTS

The authors acknowledge the funding support from the U. S. Department of Energy (DOE) Basic Energy Sciences (LANLE3W1). We also gratefully acknowledge useful feedback from Hari Viswanathan (Los Alamos National Laboratory), Zdenek Bazant (Northwestern University), and Hoang Nguyen (Northwestern University) during discussions concerning the experiments.

REFERENCES

Bažant, Z.P. and Planas, J.: Fracture and size effect in concrete and other quasibrittle materials. Routledge. (2019)

Breede, K., Dzebisashvili, K., Liu, X. and Falcone, G.: A systematic review of enhanced (or engineered) geothermal systems: past, present and future. Geothermal Energy, 1(1), (2013), 1-27.

Frash L.P.: Optimized Enhanced Geothermal Development Strategies with GeoDT and Fracture Caging. 47th Workshop on Geothermal Reservoir Engineering, Stanford University, Stanford, California, February 7-9, (2022).

Frash, L.P., Gutierrez, M. and Hampton, J.: True-triaxial apparatus for simulation of hydraulically fractured multi-borehole hot dry rock reservoirs. International Journal of Rock Mechanics and Mining Sciences, 70, (2014), 496-506.

Frash, L.P., Gutierrez, M., Hampton, J., and Hood, J.: Laboratory simulation of binary and triple well EGS in large granite blocks using AE events for drilling guidance. Geothermics, 55, (2015), 1-15.

Fu, W., Savitski, A.A. and Bunger, A.P.: Analytical criterion predicting the impact of natural fracture strength, height and cemented portion on hydraulic fracture growth. Engineering Fracture Mechanics, 204, (2018), 497-516.

Gale, J.F., Elliott, S.J. and Laubach, S.E.: Hydraulic fractures in core from stimulated reservoirs: core fracture description of HFTS slant core, Midland Basin, West Texas. In Unconventional Resources Technology Conference, Houston, Texas, 23-25 July (2018).

Guglielmi, Y., Cappa, F., Avouac, J.P., Henry, P. and Elsworth, D.: Seismicity triggered by fluid injection–induced aseismic slip. Science, 348(6240), (2015):1224-1226.

Ishida, T., Chen, Q., Mizuta, Y. and Roegiers, J.C.: Influence of fluid viscosity on the hydraulic fracturing mechanism. J. Energy Resour. Technol., 126(3), (2004), 190-200.

Jaeger, J.C., Cook, N.G. and Zimmerman, R.: Fundamentals of rock mechanics. John Wiley & Sons, (2009).

Li, W., Frash, L.P., Carey, J.W., Meng, M., Welch, N.J. and Viswanathan, H., 2021b, December. Experimental Controls on the Transition Between Planar and Branched Hydraulic Fractures. In Unconventional Resources Technology Conference, 26–28 July (2021b), 1281-1291.

Li, W., Frash, L.P., Carey, J.W., Welch, N.J., Meng, M., Nguyen, H., Viswanathan, H.S., Rougier, E., Lei, Z., Rahimi-Aghdam, S. and Bažant, Z.P.: Injection Parameters that Promote Branching of Hydraulic Cracks. Geophysical Research Letters, 48(12), (2021a), p.e2021GL093321.

Li, W.F., Frash, L.P., Carey, J.W., Welch, N.J., Meng, M., Viswanathan, H.S., Nguyen, H., Rahimi-Aghdam, S. and Bažant, Z.P.: Effect of Injection Parameters on Hydraulic Fracture Branching. In 55th US Rock Mechanics/Geomechanics Symposium. OnePetro, (2021c).

McClure, M.W., and Horne, R.N.: An investigation of stimulation mechanisms in Enhanced Geothermal Systems. International Journal of Rock Mechanics and Mining Sciences, 72, (2014), 242-260.

Meng, M., Frash, L.P., Carey, J.W., Li, W. and Welch, N.: Rapid measurement of Biot effective stress coefficient for Class-G Oil Well Cements. In 54th US Rock Mechanics/Geomechanics Symposium. OnePetro, (2020).

Meng, M., Frash, L.P., L,i W., Welch, N.J., Carey, J.W., Morris, J., Neupane, G., Ulrich, C., Kneafsey, T.: Hydro-mechanical measurements of sheared crystalline rock fractures with applications for EGS Collab experiments 1 and 2. Journal of Geophysical Research: Solid Earth, (2022), in press.

Rahimi-Aghdam, S., Chau, V.T., Lee, H., Nguyen, H., Li, W., Karra, S., Rougier, E., Viswanathan, H., Srinivasan, G. and Bažant, Z.P.: Branching of hydraulic cracks enabling permeability of gas or oil shale with closed natural fractures. Proceedings of the National Academy of Sciences, 116(5), (2019), 1532-1537.

Renshaw, C.E. and Pollard, D.D.: An experimentally verified criterion for propagation across unbounded frictional interfaces in brittle, linear elastic materials. International journal of rock mechanics and mining sciences & geomechanics abstracts, 32(3), (1995), 237-249.

Rinaldi, A.P. and Rutqvist, J.: Joint opening or hydroshearing? Analyzing a fracture zone stimulation at Fenton Hill. Geothermics, 77, 2019, 83-98.

Taleghani, A.D.: Fracture re-initiation as a possible branching mechanism during hydraulic fracturing. In 44th US Rock Mechanics Symposium and 5th US-Canada Rock Mechanics Symposium. OnePetro, (2010).

Tan, P., Jin, Y., Han, K., Hou, B., Chen, M., Guo, X. and Gao, J.: Analysis of hydraulic fracture initiation and vertical propagation behavior in laminated shale formation. Fuel, 206, (2017), 482-493.

Weng, X., Kresse, O., Cohen, C.E., Wu, R. and Gu, H.: Modeling of hydraulic fracture network propagation in a naturally fractured formation. In SPE Hydraulic Fracturing Technology Conference. Society of Petroleum Engineers, (2011).